

UPTEC X 02 037  
DEC 2002

ISSN 1401-2138

EVA-LENA ENGMAN

# Image processing using statistical tools in the diagnosis of dementia

Master's degree project



**Molecular Biotechnology Programme**  
**Uppsala University School of Engineering**

<b>UPTEC X 02 037</b>	<b>Date of issue 2002-12</b>	
Author <b>Eva-Lena Engman</b>		
Title (English) <b>Image processing using statistical tools in the diagnosis of dementia</b>		
Title (Swedish)		
Abstract Three methods for quantitative analysis of brain changes in dementia were developed in ANSIC. The correlation method computes the correlation between a neuropsychological test and the local cerebral blood flow for each volume element of the brain. The Cavalieri stereology method calculates the volume of tissues in the brain. The Fuzzy clustering algorithm classifies every image volume element to a predefined tissue class.		
Keywords Image processing, dementia, SPECT, MRI, atrophy, cerebral blood flow, correlation, stereology, fuzzy clustering		
Supervisors <b>Leif Svensson</b> <b>Per Julin</b> <b>Huddinge University Hospital / Karolinska Institutet</b>		
Examiner <b>Bert Sarby</b> <b>Huddinge University Hospital / Karolinska Institutet</b>		
Project name	Sponsors	
Language <b>English</b>	Security	
<b>ISSN 1401-2138</b>	Classification	
Supplementary bibliographical information	Pages <b>34</b>	
<b>Biology Education Centre</b> Box 592 S-75124 Uppsala	<b>Biomedical Center</b> Tel +46 (0)18 4710000	<b>Husargatan 3 Uppsala</b> Fax +46 (0)18 555217

# **Image processing using statistical tools in the diagnosis of dementia**

**Eva-Lena Engman**

## **Sammanfattning**

Vid demens, som till exempel Alzheimers sjukdom, sker det förändringar i hjärnans vävnader. Bland annat så ersätts hjärnceller som dött och transporterats bort från hjärnan med vätska. Dessa förändringar kan man titta på med hjälp av olika metoder. Här har tre olika metoder utvecklats i programmeringsspråket ANSI C för att se hur stora förändringarna i hjärnan blir hos en patient med demens.

Den första metoden används för att se om det finns någon relation mellan ett psykologiskt test och blodflödet i olika delar av hjärnan. Blodflödet är nämligen proportionellt mot aktiviteten i de olika områdena. Skadade delar av hjärnan har lägre aktivitet och därmed lägre blodflöde. Personer som har skador i hjärnan som kommer av demenssjukdomen har lägre resultat på de psykologiska testet.

Den andra metoden används för att mäta olika volymer i hjärnan. På så sätt kan man se om delar av hjärnan har dött och ersatts med vätska.

Den tredje metoden bestämmer vilken sorts vävnad varje liten del av hjärnan tillhör. Genom denna segmentering kan man även volymsbestämma olika vävnader, här sker detta dock mer automatiskt än i metod två.

**Examensarbete 20 p i Molekylär bioteknikprogrammet  
Uppsala universitet december 2002**

# Contents

<b>1</b>	<b>Introduction</b>	<b>5</b>
1.1	General . . . . .	5
1.2	Dementia . . . . .	5
1.3	Single Photon Emission Computed Tomography (SPECT) . . . . .	7
1.4	Magnetic Resonance Imaging (MRI) . . . . .	8
1.5	Implementation. . . . .	11
<b>2</b>	<b>Correlation analysis</b>	<b>12</b>
2.1	Introduction . . . . .	12
2.2	Material and methods . . . . .	12
2.3	Result . . . . .	15
2.4	Discussion . . . . .	15
<b>3</b>	<b>Volume analysis</b>	<b>17</b>
3.1	Introduction . . . . .	17
3.2	Material and methods . . . . .	17
3.3	Result . . . . .	20
3.4	Discussion . . . . .	24
<b>4</b>	<b>Cluster analysis</b>	<b>25</b>
4.1	Introduction . . . . .	25
4.2	Material and methods . . . . .	26
4.3	Result . . . . .	28
4.4	Discussion . . . . .	30
<b>5</b>	<b>General discussion</b>	<b>31</b>
<b>6</b>	<b>Acknowledgements</b>	<b>32</b>
<b>7</b>	<b>References</b>	<b>32</b>

# 1 Introduction

Due to methods available today for brain imaging, it has become possible to quantify brain changes related to dementia. In the future, this might have an impact on early diagnosis and also treatment evaluation. In this study, three methods have been developed for quantitative analysis of brain changes.

The regional cerebral blood flow (rCBF) is reduced in certain areas of the brain in subjects with dementia. In the correlation analysis method, the local blood flow in patients with Alzheimer's disease and patients with cognitive impairment was correlated to the result these patients had on a neuropsychological test. It is then possible to see the relation between symptoms and changes in the blood flow in dementia.

The extent of atrophy in the brain, that is, the reduction of brain volume, is higher in patients suffering from dementia than in normal subjects. This atrophy can be seen in magnetic resonance images. The Cavalieri stereology method is a direct method for measuring volumes of different tissues in the brain.

Fuzzy cluster analysis is a method that automatically measures the volumes of grey and white matter as well as the volume of e.g. lesions. It does so by classifying every image volume element (voxel) as belonging to a certain (predefined) tissue class.

The three different methods are treated separately in this report but are discussed together under "5 General discussion".

## 1.1 General

The amount of people suffering from moderate to severe dementia in Sweden is estimated to be around 100.000 [1]. Due to the increase in human life length, dementia is an increasing burden in the society, socially and economically. The costs are in level of those for cardiovascular diseases [2]. Progresses in dementia diagnosis and treatment can therefore give large positive economic consequences.

## 1.2 Dementia

There are many different types of dementia. Some of the major disorders causing dementia are degenerative diseases (e.g. Alzheimer's Disease, Pick's Disease), vascular dementia (e.g. Multi-infarct Dementia), anoxic dementia (e.g. Cardiac Arrest), infectious dementia (e.g. Creutzfeldt-Jakob Disease) and toxic dementia (e.g. Alcoholic Dementia) [2]. Up to 50 % of all cases of dementia are diagnosed as Alzheimer's disease [3].

Research has established a probable model how the brain typically is damaged by Alzheimer's disease: In the brain regions attacked by Alzheimer's disease, the nerve cells degenerate and lose their connections with other nerve cells. Some nerve cells die. This degeneration starts in the entorhinal cortex and proceeds to the hippocampus. As the hippocampal nerve cells degenerate, short-term memory falters and the ability to perform routine tasks begin to deteriorate as well. Alzheimer's disease then gradually spreads to other regions, particularly the cerebral cortex. This is the outer area of the brain, which is involved in functions such as language and reason, and in its final stage Alzheimer's disease wipes out the ability to communicate or to recognise even close family members [2, 4]. Hallmarks in Alzheimer's disease include neuritic plaques and neurofibrillary tangles and these are in centre of researchers attention today. There are some hypothesis why Alzheimer's disease arises, for instance, that it is caused by a genetic disorder, a virus or some toxic substance [4].

Pick's disease is a progressive dementia with an outbreak earlier than Alzheimer's disease. It results in slow changes in character leading to impairment of intellect, memory and language. The personality changes and the person may lose his or her inhibitions. Where Alzheimer's disease generally affects most of the brain, Pick's disease affects the frontal and temporal lobes which atrophies. In addition, brain cells in these areas sometimes are found abnormal and swollen. These cells are the hallmarks of Pick's disease and are called Pick's cells [5, 6].

A way of detecting dementia is by looking at the regional cerebral blood flow (rCBF) (Figure 1). This is because the blood flow in different parts of the brain is strongly coupled to the degree of activity. A low activity requires less oxygen and glucose and, hence, the blood flow to that area is low. The reduced rCBF in dementia most likely reflects a reduced number of nerve cells and a reduced nerve cell function. In Alzheimer's disease there are often reductions in the rCBF temporally, which can be seen at an early stage of the disease (Figure 1 b). In frontal-lobe dementia (Pick's disease) the blood flow is highly reduced frontally bilaterally (Figure 1 c). Changes in rCBF can sometimes be found before a patient fulfil the criteria for dementia and before morphological changes can be seen with e.g. magnetic resonance imaging [7].

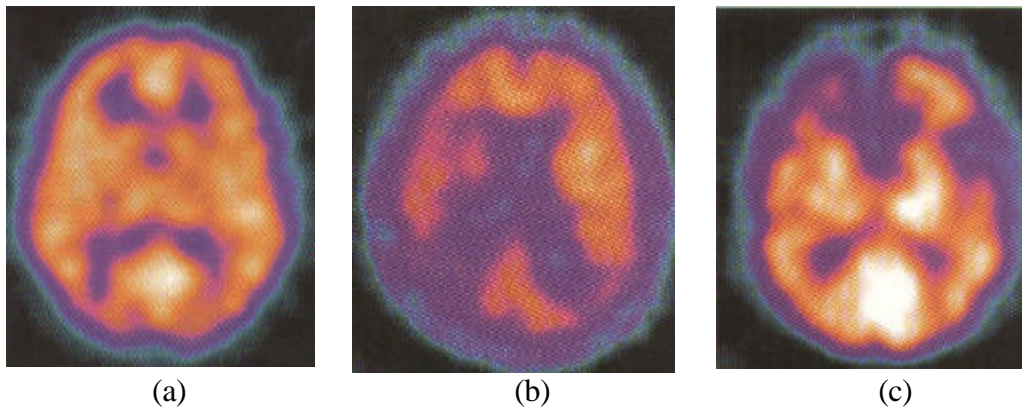
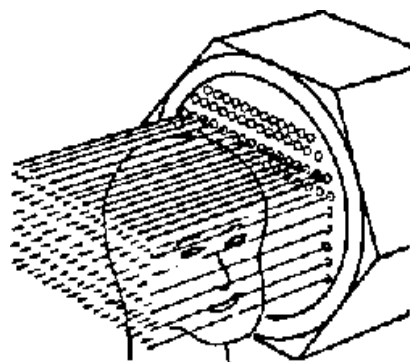


FIGURE 1[7]:The regional cerebral blood flow (rCBF) measured with SPECT. A healthy subject (a), a subject with signs of Alzheimer's disease (b) and a subject with Pick's disease (frontal-lobe dementia) (c).

### 1.3 Single Photon Emission Computed Tomography (SPECT)

In SPECT technology the patient is injected with a radiopharmaceutical emitting gamma rays which will be collected by a gamma camera. When measuring the regional cerebral blood flow (rCBF) in the brain a useful labelled isotope is  $^{99}\text{Tc}^m$ -HMPAO. This compound is fat-soluble and therefore easily crosses the blood-brain barrier. Inside the brain the compound is converted to a water-soluble form and can not pass back over the blood brain barrier. This makes it possible to “freeze” a moment of brain activity. The compound is distributed in the brain approximately proportional to the regional blood flow.  $^{99}\text{Tc}^m$  has a half live of about six hours and the emitted photon of 140 keV is easily detected by gamma cameras.



The gamma camera has three basic layers – a collimator, a crystal and a detector. The collimator is usually made of lead and contains thousands of parallel channels through which gamma rays are allowed to pass. These holes only allow the gamma rays which are perpendicular to the plane of the camera to enter (Figure 2), which makes it possible to reconstruct the image.

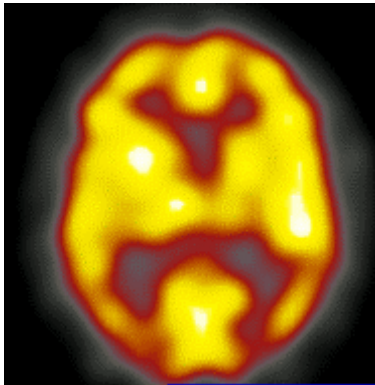
FIGURE 2 [8]:The collimator is perpendicular to the camera, allowing only perpendicular gamma rays to pass.

The collimator is placed directly on top of a single crystal of NaI. Gamma rays travelling along a path that coincides with one of the collimator channels will pass through the collimator unabsorbed and interact with the NaI crystal. Gamma rays hitting the crystal will be transformed into light

rays, which are amplified and transformed into electrical impulses by a grid of photomultipliers behind the crystal [9].

In SPECT, the gamma camera is rotated 360 degrees around the part of the body being investigated. The camera stops at equally spaced angles collecting data. Because of this, a computer can construct a three dimensional image of the area [8].

The achieved data must be corrected for attenuation, which causes a reduction in the number of photons reaching the camera. The photon can be prevented from reaching the detectors either by scattering or absorption by an atom or a molecule. The amount of attenuation experienced by a photon depends on its path through the body and its energy [9].



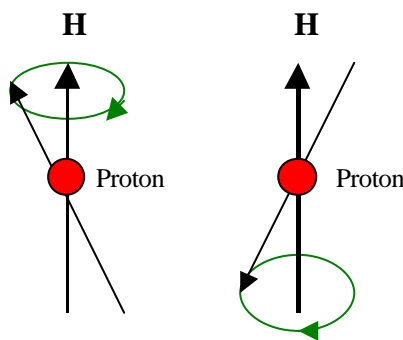
SPECT images give information associated with radioactive tracer behaviour relative to cerebral blood flow but are lacking in finer anatomic detail (Figure 3).

FIGURE 3: *SPECT image showing regional cerebral blood flow (rCBF) in the brain.*

## 1.4 Magnetic resonance imaging (MRI)

Most kinds of atomic nuclei possess a small magnetic moment. Hydrogen has the simplest nucleus, a single proton and, since it is the most abundant nucleus in the body and its magnetic moment is large, it emits by far the strongest MR signal of all nuclei.

Under normal circumstances, the magnetic moments of the nuclei have



random orientation which varies rapidly as a result of thermal motion. When placed in a magnetic field, however, the magnetic moments will be orientated either with or against the field direction with a preference for the with H orientation.

FIGURE 4: *Proton orientation and spin in a magnetic field H.*

The alignment with the field is not perfect and the magnetic moments of the protons spin around the direction of the magnetic field (Figure 4). The frequency of this spin depends on the isotope involved and the magnetic field at the site of the nucleus according to the equation:

$$w_l = g \times H$$

where  $\omega_l$  is the Larmor frequency (MHz),  $\gamma$  a constant for the nucleus involved and  $H$  is the magnetic field strength (Tesla) [10].

The direction of the protons themselves give rise to a small magnetisation  $M(t)$  (Figure 5 a), but it is too weak to be measured directly in a strong magnetic field. However, if  $M(t)$  is deviated  $90^\circ$  by applying a radio frequency (RF) pulse of short duration at the Larmor frequency a different situation arises;  $M(t)$  then rotates at the Larmor frequency around the field direction. If a coil is put next to or around the object being measured, the rotating magnetisation evokes an alternating current at the Larmor frequency in the coil, which functions as an antenna (Figure 5 b). This is the MR signal, and the strength of the signal is proportional to the magnetisation  $M(t)$ . The magnetisation  $M(t)$  goes back to be aligned with the magnetic field  $H$  through two different relaxation processes,  $T_1$  and  $T_2$ . Depending on these parameters, and when the coil starts receiving signal from the object, the so called echo-time, it is possible to construct images with different contrast and different tissue separation – different MR sequences. For instance, images showing proton density (short echo-time),  $T_1$ - and  $T_2$ -weighted images can be constructed. If the RF pulse that is supposed to flip the magnetisation  $M(t)$  from the direction of the magnetic field does not have a frequency that closely matches the Larmor frequency, the magnetisation remains aligned with the field and no MR signal is obtained.

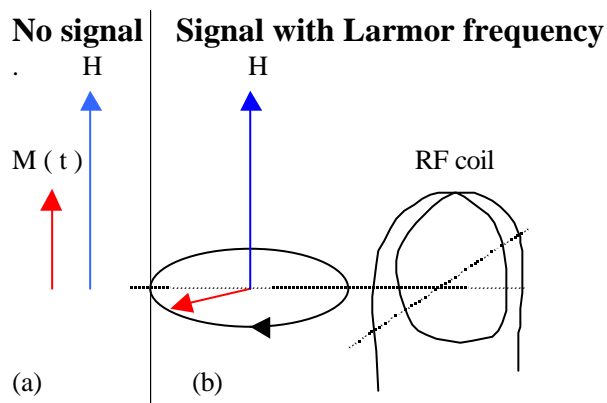


FIGURE 5: *The protons give rise to a small magnetisation  $M(t)$  when put in a large magnetic field  $H$  (a). When a RF pulse at the Larmor frequency is applied,  $M(t)$  is deviated  $90^\circ$  and rotates at the Larmor frequency about  $H$ 's field direction. A coil put next to the*

*object will show an alternating current at the Larmor frequency. (b)*

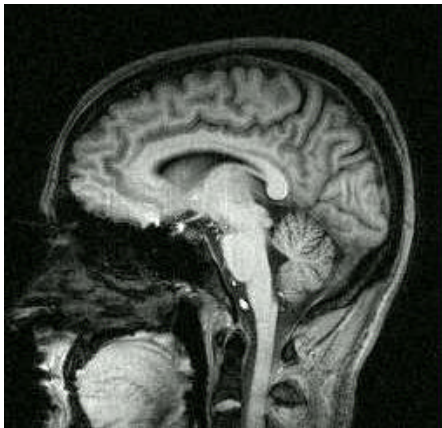
So, what does the signal tell us? The Larmor frequencies of individual protons depend on the specific position of protons within a molecule, what kind of molecule they are part of and the strength of the magnetic field they are experiencing. For example, there is a small difference in frequency between protons in  $\text{CH}_3$  groups and OH groups and a difference between protons in water and fat. These variations are due to the presence of the electrons surrounding the atomic nuclei. Electrons establish a weak shield against the externally applied magnetic field which is decreased at the site of the proton. The level of shielding depends on the amount of electrons surrounding the proton. Thus, protons in different kinds of molecules or occupying different positions within the same molecule emit their signals at

shifted frequencies, this is known as a chemical shift. Consequently, the MR signal contains a spectrum of frequencies instead of being a signal at just a single frequency [10].

How do we know where a signal is coming from? The Larmor frequency of the MR signal increases with the strength of the magnetic field.

Consequently, in the hypothetical situation where the magnetic field differs for each image volume element (voxel) within the volume of the patient, the frequency of the signal will also differ for each voxel. The summed signal of all voxels, measured by the coil outside the patient, would then be built up of components of different frequencies. This complex signal can be decomposed into its components by Fourier transformation. In the case of all voxels having a different frequency, a Fourier transformation of the total signal would reveal the contribution from each voxel to the signal which could then be displayed as an image [10].

To get a 3D volume, several slices of the object is imaged. To be able to select a certain slice for excitation, a weak inhomogeneous field is superimposed on the main magnetic field with the help of supplementary coils. The extra field can be tailored to increase in strength in any direction, for example along the axis of the patient. In the presence of the gradient, every axial cross section of the patient has its own Larmor frequency. To turn the magnetisation perpendicular to the magnetic field, a  $90^\circ$  RF pulse that closely matches the Larmor frequency is applied. Consequently, if an RF pulse with a narrow range of frequencies centred around a central peak is applied in the presence of the gradient, only a narrow band of protons will respond and only the magnetisation within that band will be turned perpendicular to the field and produce a signal in the detection coil. This is called slice-selective excitation. A different slice is selected by choosing a different peak frequency of the RF pulse or by moving the gradient field. The thickness of the slice and the steepness of the edges are determined by the strength of the gradient, and the range of frequencies present in the RF pulse: the bandwidth. If the frequency range is narrow, the slice is thin. This can also be achieved by applying a stronger gradient so that for a given range of frequencies in the RF pulse, a smaller part of the subject is selectively excited [10].



MRI provides images of the brain which are rich in anatomic detail. It has the capability to image different tissue types, for instance, grey and white matter in the brain can be contrasted from each other (see Figure 6) [11].

FIGURE 6 [12]: *An MR image showing, with great detail, a sagittal slice of the brain.*

## **1.5 Implementation**

The programs were implemented in UNIX environment, operative system Solaris 5.6 from SUN. All code was written in ANSI C and was compiled with the GNU C compiler. The program was written and executed on a Hermes workstation, Nuclear Diagnostics. The correlation method and clustering method were added to an existing program called Volume Statistics, and the volume measuring program was added to a program called Dmr. Both the Volume Statistics program and the Dmr programs has been developed at the Department of Hospital Physics, Huddinge University Hospital.

## 2 Correlation analysis

### 2.1 Introduction

The preclinical stage of Alzheimer's disease (AD) can be described using a term called mild cognitive impairment (MCI). A person with MCI can e.g. have mild memory disorders not severe enough to be diagnosed as dementia. Subjects with MCI develop AD with a rate ten times the rate for a normal subject. It is of great interest to, at an early stage as possible, separate subjects with progressive mild cognitive impairment (PMCI), that is, subjects that converts to AD, from those subjects with stable (non-progressive) mild cognitive impairment (SMCI). If there is an early onset of medication, it is more likely to have effect, and could thereby reduce the social and economic costs [13].

The function of the nerve cells are closely coupled to the local blood flow. If the nerve cells get damaged e.g. at nerve cell death in Alzheimer's disease, this region will require less or no blood flow [2]. Measuring the regional cerebral blood flow (rCBF) it is possible to see if regions in the brain have been damaged and thereby lost or decreased their blood flow, and where these regions are located.

Since it is possible to align SPECT images with each other, it is also possible to compare image voxels in one image with the corresponding voxels in another image. There have been many activation studies where voxels in the same position in different images have been compared [14]. In these kinds of studies, the subjects usually gets a task like moving their hand or looking at images. Then the voxels are compared to the voxels in an image where the subject was resting, to see what parts of the brain are activated when doing the task. There have also been some studies, as in this one, where only one image has been taken of each subject, and the voxels are being compared to something else. In this study, the regional cerebral blood flow was compared with a neuropsychological test.

Different markers are used to detect dementia, e.g. neuropsychological tests. These cognitive tests can give hints to which type of dementia the subject has [4]. By comparing these test with the blood flow in the brain it could be possible to find regions where the blood flow is correlated to the subjects result on the test. This could be useful to understand the relation between cognitive impairment and brain changes in early dementia.

### 2.2 Material and methods

#### *Subjects*

37 subjects diagnosed as MCI that have been under investigation for suspected dementia at the geriatric clinic, Huddinge University Hospital, and 14 subject already diagnosed as AD patients, were used in the trial. At

the first time of investigation the MCI subjects had performed at least 1.5 standard deviations below average for their age on at least one neuropsychological test but did not fulfil the criteria of dementia according to DSM-IV criteria [15]. The subjects have been followed for a time of  $28.9 \pm 16.3$  months on average. After this time, the subjects still had not fulfilled the criteria for dementia and were considered stable (SMCI) [13].

### ***Neuropsychological Tests***

The neuropsychological test used for the correlation analysis was a minimal state examination, MMSE, developed for diagnosis of patients with dementia. The test consists of 30 different tasks, such as remembering three words, drawing a figure, etc.

### ***Single Photon Emission Computed Tomography (SPECT)***

1000 Mbq Tc-99m-HMPAO was injected into each patient in a resting state. Resting state means that the subject had been resting in a dark room for about 30 minutes. The injection was done with the subjects eyes closed. This is important since the rCBF is proportional to the activity in the brain. The SPECT examination started 30 minutes after injection and were performed with a single headed Siemens Diacam gamma camera. The subjects were scanned in 64 projections at regular intervals around the head (360 degrees). The spatial resolution of this camera is 10.2 mm (FWHM). Reconstruction of the tomographic slices was made with an iterative algorithm (Hosem, Nuclear Diagnostics AB, Sweden) with attenuation correction according to Chang (attenuation coefficient ( $0.12\text{cm}^{-1}$ )). The data was stored in a  $64 \times 64 \times 64$  dataset matrix with a cubic voxel size of 3.5 mm. 3D image filtration was made with a Butterworth filter, cutoff  $0.7\text{ cm}^{-1}$  [13].

### ***Registration***

The data from the subjects were registered using the BRASS software developed by Nuclear Diagnostics with 9 parameter linear registration to a normal template. As similarity function the normalised mutual information was used. After this the subjects brains are all aligned and adjusted to the region map, which contains 46 volumes of interest. (see Figure 7) [16].



FIGURE 7: A transversal slice of the region map which contains 46 volumes of interest

### ***Normalisation***

The voxel values of each subject were normalised to the Cerebellum by dividing each voxel value by the mean pixel value of the Cerebellum of that subject. The Cerebellum was chosen for normalisation because its blood flow normally stays intact at dementia.

### **Correlation**

Correlation shows how well data points  $(a_i, b_i)$  can be fitted to a line. For example, if the length of some persons and the number of hairs on their heads were to be compared, there would probably not be any relationship found between the two variables, the data would spread out in 2D space and it would be hard to fit to a line to the data. But if the length of some persons was compared to the weight of those persons, a relation between the variables would be found; the variables are said to be correlated.

The correlation for the different neuropsychological tests versus the voxel value within the region map was calculated according to the formula:

$$r(x, y, z) = \frac{N \sum a_i b_i - \sum a_i \sum b_i}{\sqrt{N \sum a_i^2 - (\sum a_i)^2} \sqrt{N \sum b_i^2 - (\sum b_i)^2}} \quad (2)$$

where  $a_i$  is subject  $i$ :th voxel value in position  $(x, y)$  in image  $z$ ,  $b_i$  is the neuropsychological test value for subject  $i$  and  $N$  is the number of subjects in the study. The correlation value  $r$  ranges from zero, when there is no correlation, to  $\pm 1$ , where there is complete correlation [17].

The p-value was calculated for each correlation value, that is, for each voxel, with the betai function described in [18]. The t-value used in the function was:

$$t = r(x, y, z) \sqrt{\frac{N - 2}{1 - r(x, y, z)^2}} \quad (3)$$

where  $r$  is the correlation and  $N$  is the number of subjects in the study [18]. The p-value is the significance level at which the hypothesis that the correlation calculation is correct is disproved.

### **Region growth**

The voxel value with the largest absolute correlation  $r(x, y, z)$  with a p-value  $< 0.05$  was “grown” by adding pixels next to it, also with a p-value  $< 0.05$ . New pixels were added until the absolute value of the correlation for all the pixels in this grown region reached a lower limit, which was chosen to be 0,6. The new correlation value was calculated according to Equation 2. This procedure was repeated until a certain amount of grown regions had emerged. A reason for growing regions is that it always is a statistical possibility for a voxel to show a high correlation although there is not any. By growing voxels together, the chance for this mass-significance error to occur is minimised.

## 2.3 Results

The correlation between the rCBF and the MMSE test in the 51 subjects, 14 AD and 37 SMCI, shows an absolute correlation value larger than 0.6 in the temporo-parietal regions in the brain (Figure 8). These regions couples different modalities from e.g. vision, hearing and feeling to an understandable entity. These results are expected, due to the composition of the MMSE test and are also consistent with other studies of regions effected by Alzheimer's disease.

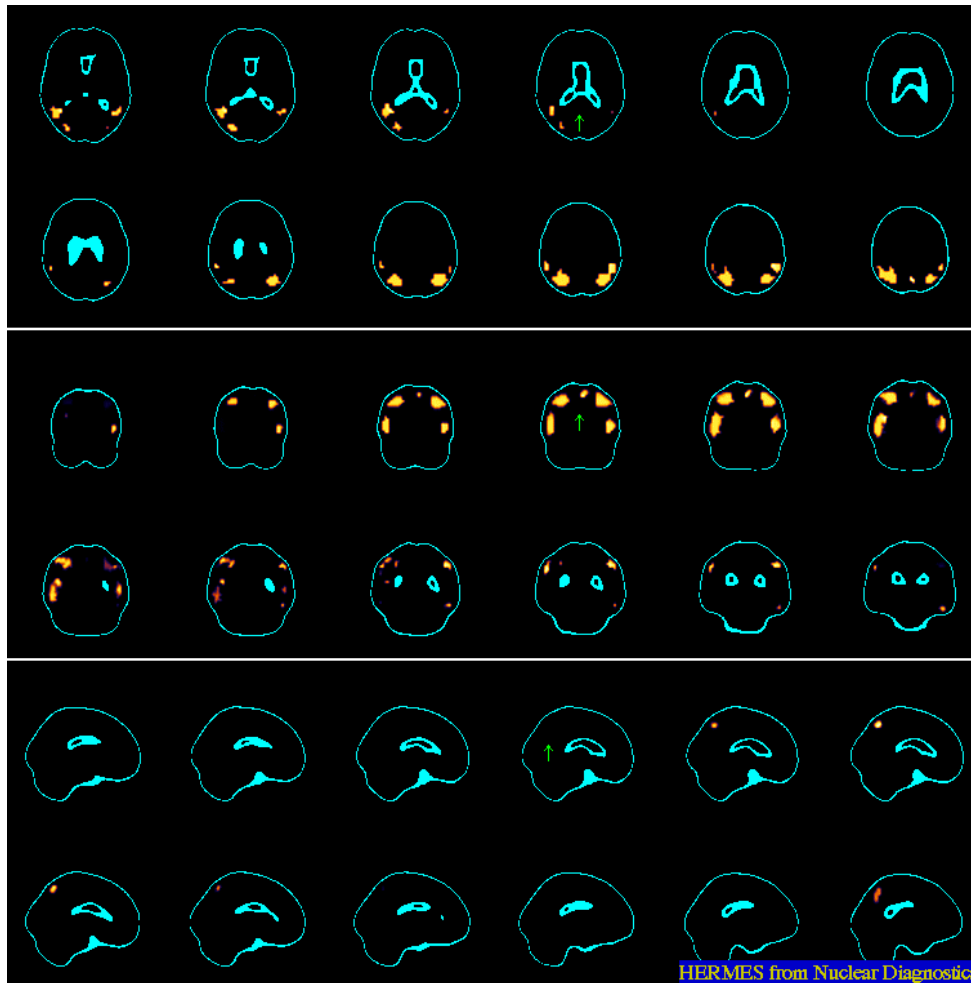


FIGURE 8: *The correlation between the rCBF and a MMSE test in 51 subjects, 14 AD and 37 SMCI. The grown regions with a absolute correlation value larger than 0.6 are shown in yellow in the reference brain (blue boarders). Brain regions effected are temporo-parietal association areas. The green arrow points at the same voxel in the transversal, coronal and sagital cross-sections.*

## 2.4 Discussion

The correlation analysis method can be used with any cognitive test. If a subject has a bad result on some cognitive test, then the regions in the brain

that are used while solving the test might also have a lowered blood flow. It is also possible to correlate the blood flow to e.g. the age of the subjects.

The mini-mental state examination is a quite rough test, a patient has to be quite ill to get a bad test result. The test is not primarily designed to test subjects with mild cognitive impairment. In the future, it would be interesting to test more specific neuropsychological tests, e.g. test mainly for episodic memory function.

## 3 Volume analysis

### 3.1 Introduction

Several investigations have shown that the size and shape of the brain changes in dementia. For example, in Alzheimer's patients the cerebral cortex often shows regional atrophy which is considered to be caused by the death of many nerve cells and that they together with the nerve cell outgrowths have been broken down into their chemical compounds and been transported away from the brain. In Alzheimer's disease the brain can lose up to 50 % of its weight (Figure 9) [2].

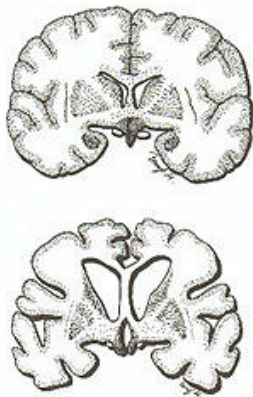


FIGURE 9: *Cross section of the brain in a normal person (upper picture) compared to a corresponding cross section from a patient that died in a late stage of Alzheimer's disease (lower picture). The mass of the tissue is comparably small, the sulci between the convolutions has expanded and the inner cavities of the brain (the ventricles) are large in patients with Alzheimer's disease [2].*

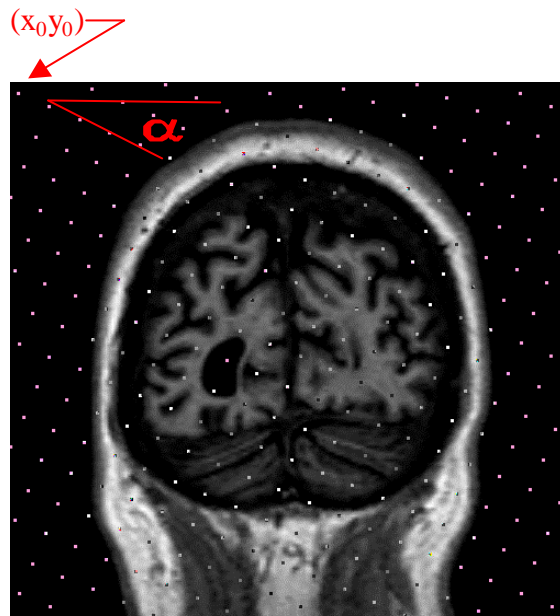
Magnetic resonance imaging (MRI) gives detailed anatomy of the brain with good image quality and it does not use ionising radiation. Many studies have shown that volumetric MRI of hippocampus and entorhinal cortex may be helpful in the diagnosis of dementia. Hippocampal atrophy may also predict the development of dementia already in patients with mild cognitive impairment (MCI). However, it is difficult to diagnose the type of dementia using hippocampal volumetry [19].

The Cavalieri method of stereology gives accurate and unbiased estimation of the volume of an arbitrary object from a few volume slices, here provided by MRI. In this investigation the Cavalieri method was used to measure the ventricle volume of an AD patient, to see if it is possible to use this method to see differences in ventricle volume over time.

### 3.2 Material and methods

The Cavalieri method is named after the Italian mathematician Bonaventura Cavalieri (1598-1647), a pupil of Galileo. He made significant advances in the mathematics of numerical integration and was the first to consider measurement of volume via the analysis of sections through three-dimensional solid objects. The method has been used many times in microscopy applications.

In the Cavalieri method a regular grid of test points with a random starting position  $(x_0, y_0)$  and orientation  $(\alpha)$  is put on each MR image (Figure 10). The function that generates the random starting position and orientation was



checked for homogeneity. The first MR image

FIGURE 10: A grid of points is put onto each chosen MR image, with a random starting point  $(x_0, y_0)$  and a randomly chosen angle  $(\alpha)$ . Each point hitting the structure of interest is counted on each MR image and the area can be calculated by multiplying the amount of points with the area associated with each point..

should be randomly chosen and the images parallel a constant distance apart (Figure 11). Because the subjects position in the camera varies from person to person the position of the first image will automatically become random.

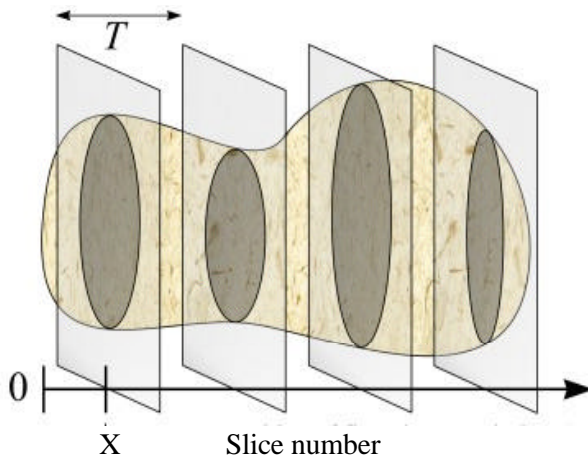


FIGURE 11[20]: Volume estimation using the Cavalieri method. The first slice has a random start position  $X$  and the slices are separated by a constant distance  $T$ . The volume is calculated by multiplying the area of interest in each slice with the slice interval  $T$ .

After each superimposition, the number of test points hitting the structure of interest is counted on each image, and the unbiased estimated volume becomes:

$$estV = T(P_1 + P_2 + \dots + P_n)A$$

(4)

where  $T$  is the distance between the images,  $P_1, P_2, \dots, P_n$  is the amount of counted points on each image and  $A$  is the area associated with each point [21].

A reasonable, but not mathematically unbiased error prediction formula, was proposed by Gundersen and Jensen:

$$CE(estV) = \left( \sum_{i=1}^m P_i \right)^{-1} \sqrt{\frac{1}{12} \left( 3 \sum_{i=1}^m P_i P_i + \sum_{i=1}^{m-2} P_i P_{i+2} - 4 \sum_{i=1}^{m-1} P_i P_{i+1} \right)} \quad (5)$$

where  $P_i$  is the amount of points counted in the  $i$ :th layer [21].

The orientation of the test system does not effect unbiasedness. However, if one wants to predict the error of a Cavalieri estimate of volume with the formula above (Equation 5), then it is necessary to use new random starting positions and orientation on each section [21].

For an object of volume  $V$  with a distance  $T$  between the planes, the required distance between the test points of the grid to get a small error in the estimation of the volume, is, according to [22]:

$$d = \sqrt{\frac{V}{100 * T}} \quad (6)$$

To test the Cavalieri stereology program, a vinyl exam glove was filled with 200 ml water and 0.3 ml gadolinium contrast and was put in two different configurations in the MR machine and  $T_1$ -weighted images were acquired. The two different sets of images were run in the Cavalieri stereology program with different slice and test point distances to see if the program was running properly and to see how many points it is necessary to count in order to get a good estimate of the volume.

Six persons, each with two different MR scans a week apart, were run in the stereology program, twice for each scan. A repeated Anova test was made to see what the method error was in the scan and in the Cavalieri stereology method. The first picture to be measured was also varied, to see if this effects the volume, as well as the slice interval.

The ventricular volume of an AD patient was measured twice 22 months in between to see if there was any significant change in the ventricle volume.

### 3.4 Results

The volume of 200 ml water in a vinyl exam glove in two different configurations was estimated seven times with the Cavalieri stereology method according to Table 1 and 2.

Estimated volume	CE(estV)	True error	Test point distance	Image interval
201.0 cm <sup>3</sup>	2.3%	0.5%	1.8 cm	0.5 cm
200.0 cm <sup>3</sup>	2.5%	0%	1.8 cm	0.5 cm
201.4 cm <sup>3</sup>	1.8%	0.7%	2.0 cm	0.4 cm
200.1 cm <sup>3</sup>	9.4%	0.1%	2.6 cm	1.0 cm
199.4 cm <sup>3</sup>	9.8%	0.3%	2.6 cm	1.2 cm
198.7 cm <sup>3</sup>	16%	0.7%	2.6 cm	1.3 cm
182.1 cm <sup>3</sup>	15%	9.8%	3.0 cm	1.2 cm

TABLE 1: Configuration 1. The mean value of the volume is 197.5 cm<sup>3</sup> and the standard deviation is 6.85 cm<sup>3</sup>. All volumes lies within the estimated error (CE(estV)) from Equation 5. The “true error” is the deviation of the estimated volume from the true volume of 200 cm<sup>3</sup>.

Estimated volume	CE(estV)	True error	Test point distance	Image interval
200.2 cm <sup>3</sup>	2.5%	0.1%	1.8 cm	0.5 cm
205.0 cm <sup>3</sup>	1.8%	2.5%	1.8 cm	0.5 cm
201.7 cm <sup>3</sup>	2.4%	0.9%	1.9 cm	0.5 cm
199.0 cm <sup>3</sup>	2.0%	0.5%	2.3 cm	0.5 cm
199.8 cm <sup>3</sup>	1.7%	0.1%	2.7 cm	0.5 cm
203.3 cm <sup>3</sup>	7.8%	1.7%	3.1 cm	1.0 cm
201.0 cm <sup>3</sup>	50%	0.5%	2.7 cm	3.0 cm

TABLE 2: Configuration 2. The mean value of the volume is 201.3 cm<sup>3</sup> and the standard deviation is 2.33 cm<sup>3</sup>. All volumes except number two lies within the estimated error (CE(estV)) from Equation 5. The “true error” is the deviation of the estimated volume from the true volume of 200 cm<sup>3</sup>.

It is possible to vary the image interval and the test point distance some without losing accuracy. The estimated error is often much larger than the true error, making the estimated error a worst-case scenario.

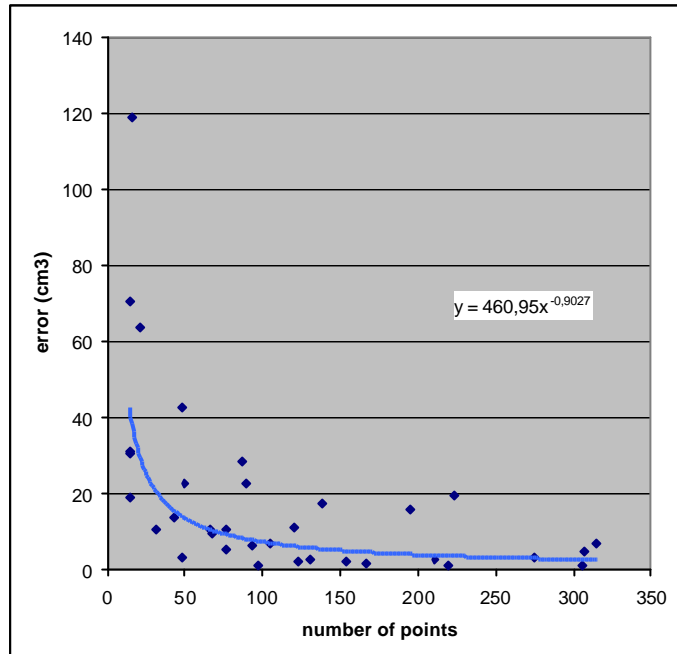


DIAGRAM 1: *The program was tested several times with a glove filled with water. The estimated value was compared to the real value of 200 ml. The absolute value of the estimated value minus the real value is plotted against the number of points that were hitting the region of interest and a curve is fitted to the values. Both*

*the image interval and the test point distance were varied.*

Diagram 1 shows that for measuring the glove with 200 ml water, there should be at least 250 points counted to get an accurate estimate of the volume. Depending on the shape of the object, the same volume might need different amount of points to be counted to get a good estimate of the volume.

Six young healthy persons were scanned twice in the MR machine and their intracranal volume was measured twice for each person and scan with the Cavalieri stereology method, see Table 3.

Subject	1 <sup>st</sup> time Volume (cm <sup>3</sup> )	2 <sup>nd</sup> time Volume (cm <sup>3</sup> )
C scan nr 1	1447.04	1451.52
C scan nr 2	1435.85	1411.20
K scan nr 1	1258.88	1256.64
K scan nr 2	1236.48	1256.64
L scan nr 1	1435.20	1456.80
L scan nr 2	1459.20	1444.80
M scan nr 1	1432.80	1413.60
M scan nr 2	1471.20	1416.00
P scan nr 1	1485.60	1497.60
P scan nr 2	1413.60	1404.00
S scan nr 1	1456.80	1464.00
S scan nr 2	1440.00	1464.00

TABLE 3: *The intracranal volume measured with the Cavalieri stereology method of six young healthy subjects, each scanned twice. The volume was calculated twice for each MR scan. A repeated Anova test shows that the largest variability lies within the MR scanning procedure. The mean value for intracranal volume of the six persons scanned twice was 1412.9 cm<sup>3</sup>.*

A repeated Anova test of the values from Table 3 shows that the largest method error is due to the MR scanning, which is 2.9%. The Cavalieri stereology method has a method error of 0.5%. The total method error of the MR scan and the Cavalieri stereology method together is 3.0%, which is smaller than the variation of 5.5% of the six healthy individuals scanned and measured. A total method error of 3.0% gives an error volume of  $1412.9 * 0.03 = 42.4 \text{ cm}^3$ . This makes it possible to separate subject C from subject K in Table 3, but it is not possible to separate subject C from subject L.

The first slice X (Figure 11) containing brain to be measured in the Cavalieri stereology method from the first scan of subject C, was varied as shown in Table 4.

Subject C scan nr 1		
First slice	Volume (cm <sup>3</sup> )	CE(estV)
1	1451.52	3.38%
2	1420.16	3.36
3	1435.84	3.25
4	1404.48	2.93
5	1395.52	3.29
6	1424.00	Lose
7	1404.48	2.89
8	1404.48	3.52

TABLE 4: *The intracranial volume was measured with the Cavalieri stereology method with a different starting image in each measurement. The mean value is  $1417.6 \text{ cm}^3$  and the standard deviation  $19.0 \text{ cm}^3$ , which indicates that the volume depends slightly on the first image chosen.*

There is a method error of 1.3% for the Cavalieri stereology method when different images are chosen as the first picture, to be compared to the method error of 0.5% when the same person was measured twice with the same start image. Choosing the 8<sup>th</sup> image as the first image might be a leap to big from the first image to get reliable results. CE(estV) (Equation 5) is independent of the first slice chosen, and therefore gives about the same value for all the measurements in Table 4.

The intracranial volume of scan number one of subject C was measured with different slice intervals, according to Table 5. The error prediction (CE(estV)) is computed from Equation 5.

Subject C scan nr 1

Slice interval	Volume (cm <sup>3</sup> )	CE(estV)
2	1394.40	0.45%
4	1412.32	1.14%
6	1421.28	1.88%
8	1447.04	3.22%
10	1428.00	4.46%
12	1344.00	6.25%

TABLE 5: *The intracranial volume of subject C's first scan. The error prediction (CE(estV)) according to Equation 5 increases when the slice distance is increased. The standard deviation is 35.8 cm<sup>3</sup>. Important to remember, though, is that the error prediction value is just a prediction, and not the actual error.*

The standard deviation of the volumes measures according to Table 5 is almost twice as high as the standard deviation when the first image to be measured was varied. This indicates that the slice interval cannot be too large if one wants to get a good estimate of the intracranial volume. The slice interval should be differently chosen depending on how small the error has to be. The smallest error is always accomplished by counting the points hitting the region of interest in every slice, that is, having a slice distance of one.

The ventricular volume of an AD patient was measured twice with a time period of 22 months in between, see Table 6.

MR scan nr 1, (cm <sup>3</sup> )	MR scan nr 2, (cm <sup>3</sup> )
72.7	96.9
73.8	97.7
77.2	91.4
77.2	98.2
78.9	96.4
80.2	97.0
74.6	98.5

TABLE 6: *The ventricle volume of an AD patient scanned twice 22 months apart. The two MR scans show significant differences in the ventricle volume, which grow more in size in AD patients than in a normal ageing subject. The mean value from scan number 1 is 76.4 cm<sup>3</sup> and the standard deviation 2.7 cm<sup>3</sup>. The mean value from scan number 2 is 96.6 cm<sup>3</sup> and the standard deviation 2.4 cm<sup>3</sup>. The first slice to be measured, the slice interval and the test point distance were all varied in the seven different volume estimations.*

The volume of the ventricles show significant differences (p-value  $1.4 \cdot 10^{-5}$ ) in the two scans. They have grown more than 25% in almost two years.

### 3.4 Discussion

The Cavalieri stereology method is useful in many applications. Humans are often more successful in detecting edges between tissue types than computers are, and are also better at getting rid of noise. It is an easy and straightforward method that does not need changes if e.g. the MR sequence is changed. Among methods with human interaction this is a faster and more reproducible method than for instance a method where one has to paint the borders of the region of interest. In the Cavalieri method, only a few points that are lying on the border of the region of interest has to be manually selected if they are supposed to be counted as well, but in the boarder painting method, every point has to be manually selected. When larger regions are being measured, one does not have to use every image in the volume to get a good estimation.

To be able to get good volume estimates the operator has to be trained, otherwise systematic errors can be introduced. Sometimes, though, due to the partial volume effect in MR images, it can be hard to know if a point should be counted or not.

One also experimentally have to test how many slices that are needed and what the test point distance should be to get a good estimation. This has to be repeated if a different kind of tissue type is being measured, due to the shape and volume of the tissue.

## 4 Cluster analysis

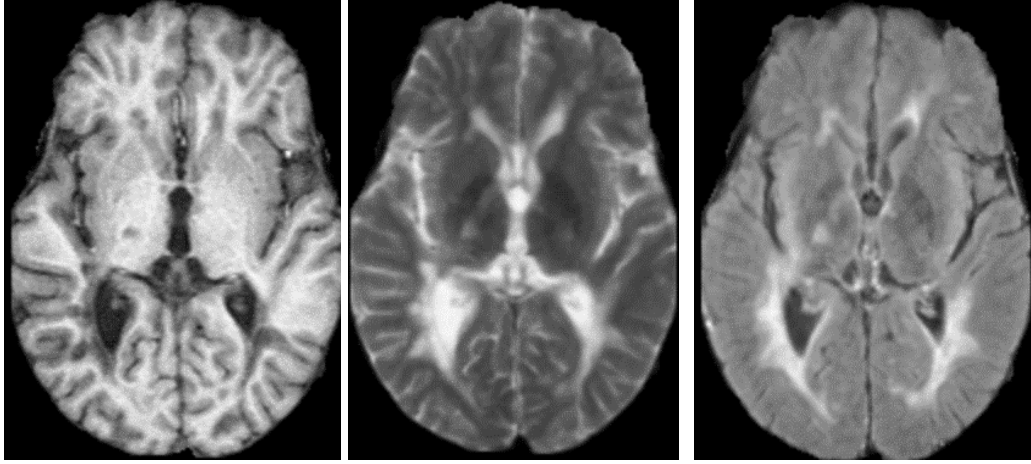
### 4.1 Introduction

The capability for accurate quantification of brain tissue volumes is of great benefit in the diagnosis, treatment and general understanding of neurodegenerative disorders. AD as well as vascular diseases and multiple sclerosis produce white matter lesions to a varying degree. A method to automatically measure not only brain but also such white matter lesions volumes would be very useful. There are several methods that have been proposed for automated or semi-automated segmentation of brain tissues and lesions from MR images. One interesting approach is to use statistical cluster analysis methods to “classify” voxels as belonging to certain (predefined) tissue classes.

Cluster analysis is a number of different classifying algorithms that organises data points into homogenous groups, or clusters. Data of the same cluster should be similar, data of different clusters should be maximally different. Assigning each data point to exactly one cluster often causes problems, because in real world problems, a certain or “crisp” separation of clusters is rarely possible due to overlapping of classes. For this reason there is a cluster analysis method called fuzzy  $c$  means classification.

The main logic behind fuzzy classification is that an object can belong simultaneously to more than a single group and does so to a varying degree. In the case of MR, grey scale voxel values in an image can, due to partial volume effects, arise from more than one tissue type, such as a combination of grey and white matter. This volume averaging of tissue poses problems for hard classification of voxels. The fuzzy  $c$ -means algorithm is a “soft” classification procedure that allow subclassification of individual MR image voxels into two or more groups. For example, a given voxel in an image could be classified as 0.4 (40%) grey matter and 0.6 (60%) white matter. Clustering algorithms, whether crisp or fuzzy, ascribe class membership to a voxel by minimising some metric of voxel to cluster centre distance. It is also a completely unsupervised method which is ideal for reasons of reliability and tractability.

It is common to simultaneously acquire more than one MR sequence during an MR scan. Using more than one image gives more information to the clustering algorithm, making it possible to do more accurate classifications [23] (Figure 12).



(a) (b) (c)

FIGURE 12: *Three different MR sequences required simultaneously. MPRAGE (a), T2-weighted (b) and FLAIR (c). This patient has multiple sclerosis, which gives lesions in the brain similar to those in Alzheimer's disease.*

## 4.2 Material and methods

To test the fuzzy  $c$ -means (FCM) segmentation algorithm, a set of pre-processed images from a patient with multiple sclerosis were available (Figure 12). All image sets were aligned to the MPRAGE image set using the multi modality software (Nuclear Diagnostics AB), with a six parameter registration with normalised mutual information as similarity measure. The extracerebral tissues in the MPRAGE image set including bone, muscle and fat was removed prior to segmentation using a region growing method with edge criteria. The resulting MPRAGE image set was used to mask the other image sequences. By doing this, the number of clusters can be reduced, since the bone, muscles etc. do not need their own cluster. The FCM algorithm makes use of iterative optimisation to approximate minima of the following fuzzy  $c$ -means function:

$$J_m(U, v) = \sum_{k=1}^n \sum_{i=1}^c (u_{ik})^m (d_{ik})^2 \quad (7)$$

where  $U$  is a fuzzy  $c$  cluster member partition of the data set  $X = (x_1 \dots x_n)$ ,  $v_i$  is the cluster centre (prototype) of class  $i$  ( $1 \leq i \leq c$ ) and  $m$  is a “fuzziness” parameter, which determines the amount of overlap between clusters ( $1 < m \leq \infty$ ) [21]. If  $m = 1$ , then the procedure is a “crisp” clustering algorithm and the membership function take discrete values only [23]. The choice of  $m$  is determined empirically based on the actual problem. The distances (Euclidean) between the data point  $k$  and the  $i$ :th cluster centre ( $v_i$ ) is [21]:

$$d_{ik}^2 = \|x_k - v_i\|^2 \quad (8)$$

First, a value for the number of clusters, the initial values for their centres, the fuzziness parameter  $m$  and the  $\epsilon$ , the stop criteria, have to be provided to start the algorithm. The initial values for the cluster centres was chosen by looking at the different tissues one wanted to get into different clusters. A neighbourhood of  $9 \times 9$  voxels was picked from one sequence and the cluster centre for that cluster and image was computed as the mean value of these  $9 \times 9$  voxels. The same  $9 \times 9$  voxels was looked up in the other sequences and the cluster centres for these images were computed in the same way. A good  $m$ -value for these application is, according to [25] 1.3, so this value was chosen.  $\epsilon$  was set to 0.01. Only the voxels with a value larger than 180 in every image was considered. This was to make the classification easier, since the liquid in the brain thereby was removed. The image sequences used were T2-weighted, FLAIR and MPRAGE (Figure 12), and three clusters were supposed to emerge from the classification; grey matter, white matter and lesions. They were all clustered one by one and than all together. The T2 image needed four clusters, since the liquid yields a high signal in those images.

Starting with  $b = 1$ , where  $b$  is the number of iterations, the iterative steps were [21]:

1. Calculation of the  $c$  cluster centres  $\{v_i^{(b)}\}$  with  $U^{(b)}$  and the formula for the  $i$ :th cluster centre:

$$v_{il} = \frac{\sum_{k=1}^n (u_{ik})^m x_{kl}}{\sum_{k=1}^n (u_{ik})^m} \quad l = 1, 2, \dots, p \quad (9)$$

where  $n$  is the amount of data points in each image and  $l$  is the image dimension.

2. Updating of  $U^{(b)}$  by calculation of the memberships in  $U^{(b+1)}$ . For  $k = 1 \dots n$ ,

- (a) calculation of  $I_k$  and  $I_k^{\sim}$ :

$$I_k = \{i | 1 \leq i \leq c, d_{ik} = \|x_k - v_i\| = 0\}, \tilde{I}_k = \{1, 2, \dots, c\} - I_k$$

- (b) For data point  $k$ , compute new membership values:  
If  $I_k = \emptyset$ :

$$u_{ik} = \frac{1}{\sum_{j=1}^c \left(\frac{d_{ik}}{d_{jk}}\right)^{2/(m-1)}} \quad (10)$$

else  $u_{ik} = 0$ .

3. The stop criteria is when the membership values have changed very little compared to the previous iteration, that is, if  $|U^{(b)} - U^{(b+1)}| < \epsilon$ , otherwise, set  $b = b+1$  and go to step 1.

After convergence a so-called “defuzzification” was invoked by assigning each voxel to the class with the largest membership value at that location. The continuous nature of the fuzzy membership is, however, useful for describing the partial volume effects within voxels of finite size and this volume was also computed and compared to the “crisp” volume. The fuzzy volume of cluster  $i$  was computed as follows:

$$Fv_i = pv \times \sum_{k=1}^n u_{ik} \quad (11)$$

where  $pv$  is the volume of each pixel and  $u_{ik}$  is the membership value of data point  $k$  to cluster  $i$ .

The crisp volume of cluster  $i$  was computed as:

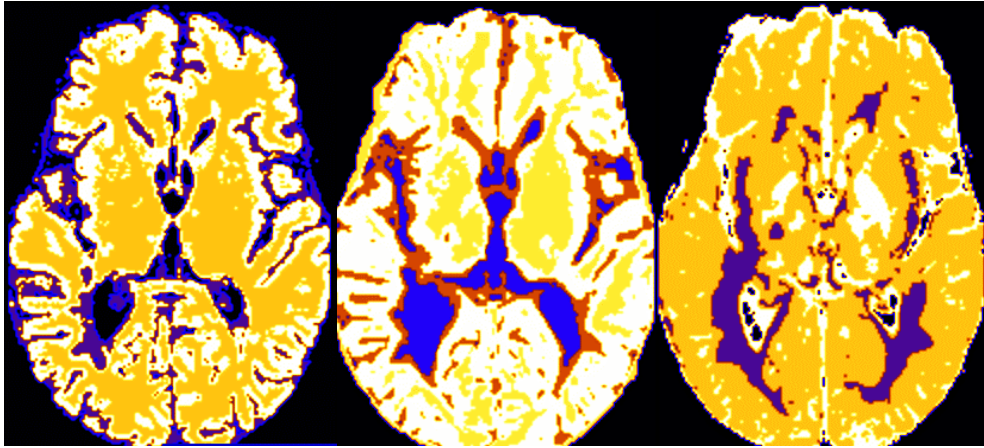
$$Cv_i = pv \times sum_i \quad (12)$$

where  $sum_i$  is the amount of pixels that have their largest membership value to cluster  $i$ .

Finally, in order to provide some verification or the accuracy of the procedure, a new image was constructed from the defuzzified (crisp) solution.

### 4.3 Results

The results from the fuzzy  $c$ -means algorithm for the three sequences (Figure 12), classified one by one are shown in Figure 13. The crisp and fuzzy volumes of the clusters for each sequence can be found in Table 7.



(a)

(b)

(c)

FIGURE 13: *The result from the Fuzzy c-means clustering algorithm for the three sequences (Figure 12) clustered one by one. (a) The clustered MPRAGE image. Lesions are shown in blue, white matter in yellow and grey matter in white. (b) The clustered T2-weighted image. Liquid is shown in blue, lesions in red, white matter in yellow and grey matter in white. (c) The clustered FLAIR-image. Lesions are shown in lilac, white matter in yellow and grey matter in white.*

The result of the Fuzzy *c*-means classified sequences (MPRAGE, T2 and FLAIR) is shown in Figure 14. The crisp and fuzzy volumes of this classification is shown in Table 7.

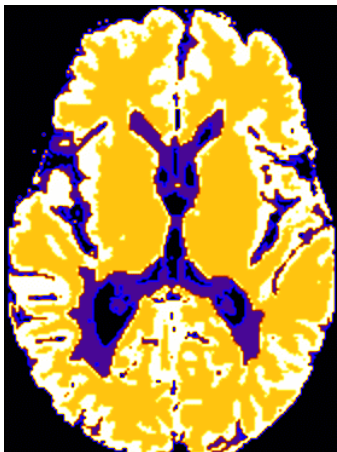


FIGURE 14: *The result from the Fuzzy c-means clustering algorithm. The lesions are shown in blue, the white matter in yellow and the grey matter in white. The non-classified voxels are shown in black.*

	Crisp volume			Fuzzy volume		
	Lesion	Grey matter	White matter	Lesion	Grey matter	White matter
MPRAGE	317	527	395	319	526	394
T2	297	782	248	297	778	252
FLAIR	120	324	852	123	324	850
All	177	513	488	177	505	496

TABLE 7: *The crisp and the fuzzy volume for the three sequences (MPRAGE, T2 and FLAIR), clustered alone and all together.*

The clustering where all three sequences were used shows the best classification of the voxels into white matter, grey matter and lesion. The lesions are much too big in the clustered MPRAGE and T2 sequences. The FLAIR sequence gives good separation of the lesions, but grey and white matter are not separated nicely. There should always be more grey matter than white matter. This is not the case in the FLAIR image. Also, the T2-weighted image contains too much grey matter. The best separated image is the one where all the images were used in the clustering. Still, the lesions are too big in this image (Figure 13). Another approach was made: The MPRAGE sequence was clustered into three clusters, white matter, grey matter and liquid. The MPRAGE sequence was chosen because it is the best of the three sequences (Figure 12) to cluster grey and white matter. This image was then weighted to have a maximum value close to the maximum value of the FLAIR sequence. The clustered MPRAGE sequence was then clustered together with the FLAIR sequence into four clusters, grey matter, white matter, liquid and lesions. The FLAIR sequence was chosen because it is the best of the three sequences to separate lesions. The result is shown in Figure 15.

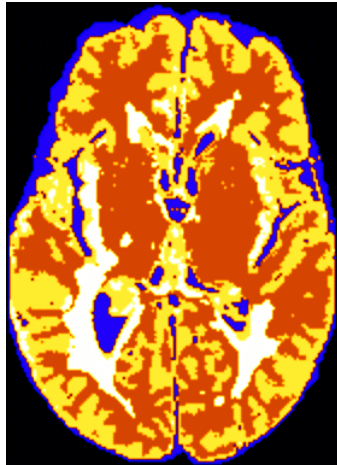


FIGURE 15: *The result from first clustering the MPRAGE sequence into three clusters, grey matter, white matter and lesions, and then clustering this image together with the FLAIR sequence. The grey matter is shown in yellow, the white matter in orange, the liquid in blue and the lesions in white.*

The fuzzy volumes from the clustering (Figure 15) was 459 cm<sup>3</sup> white matter, 602 cm<sup>3</sup> grey matter and 110 cm<sup>3</sup> lesions. The proportions grey – white matter is more reasonable than the results from Figure 14, as well as the volume of the lesions.

## 4.4 Discussion

The fuzzy clustering method is operator independent. This makes the method fast and reproducible. The method also solves, due to its “fuzziness”, the problem of partial volume effects.

The use of two or more MR sequences in the clustering procedure might give additional information and thereby a better classification. If one sequence is considered to contain more information than the other sequences used, it is also possible to weigh that one so it becomes more important than the other sequence when clustering. Using more than one sequence is not always better, if the additional sequences does not contain useful information. To give different sequences the same importance while clustering, the voxel values should be normalised. Otherwise, a sequence

with a large maximum value will affect the classification more than a picture with a small maximum value.

Depending on the clinical problem and the patient studied additional clusters would be needed to identify the presence of blood, bone, tumours, etc.

According to [26], the initial values of the cluster centres has to be within one standard deviation from the final solution in order to be certain to reach convergence. The further away the initial values of the cluster centres are from the final solution, the more iterations, and time, are required to reach the final solution.

If, as in this case, Euclidean distance is used as metric, cluster populations may tend to be equalised, which can lead to false class memberships. An idea of weighing the cluster centre positions, to account for this phenomenon, has already been introduced [23].

Due to inhomogeneity in the images it is hard to compare two different scans from the same person with each other. This might be possible after some inhomogeneity correction algorithm has been run on the images.

The MPRAGE has a very low dynamic, with a voxel maximum value of about 60. This yields a change of almost two percent if the clusters centres move one step. The dynamic can be increased through multiplication and interpolation.

There is a lot of different pre-processing that can be done to the sequences prior to cluster classification, such as filtration, correction for homogeneity, weighing the sequences or cluster centres etc. By testing and varying this pre-processing steps, it might be possible to find good clustering procedures for different applications.

## **5 General discussion**

The correlation analysis method is useful to see regions in the brain affected by Alzheimer's disease. This method needs several sets of images to get a significant result and is therefore not designed to diagnose a certain individual. But it is possible to compare a SPECT image from an ill person with the affected regions from a run of the program, to see if there are similarities.

The Cavalieri stereology method can measure tissue volumes of a single individual. This can be used e.g. to see differences in tissue volumes at two different times for the same person, or to compare the tissue volume of one individual with the average tissue volume of some population.

The cluster analysis method results in a set of images with the different tissues in the brain in different colours. It also gives the volumes of the tissues. In this way, it resembles the Cavalieri stereology method, which also gives the volumes of the tissues. The advantage of the cluster analysis method is that it is operator independent and therefore faster than the Cavalieri stereology method. The possibility to use more than one MR sequence in the clustering algorithm might also give additional information and therefore a better classification. It also solves the problem with partial volume effects better than the Cavalieri stereology method. The disadvantages of the method is that tissues of no interest, such as muscles and bone in the brain, has to be removed before the clustering takes place. Also, inhomogenities in the MR sequences makes it harder to classify correctly.

## 6 Acknowledgements

I would like to thank my supervisors Leif Svensson and Per Julin for helping me and answering all my questions, and also all the people in the Department of Hospital Physics for making my time here so pleasant.

## 7 References

- [1]. Hjärnåret. 2000. "Demens."  
[http://www3.umu.se/hjarnaret/fold\\_demens.asp](http://www3.umu.se/hjarnaret/fold_demens.asp) (25 Apr. 2002).
- [2]. Olsson, Yngve. "Alzheimers sjukdom Hjärnförändringarnas natur och uppkomst." 1999. <http://www.genpat.uu.se/popvet/yoalzheimers.html> (25 Apr. 2002).
- [3]. Nationalencyklopedin: "Alzheimers", Bokförlaget Bra Böcker AB, Höganäs, Sweden, 1989.
- [4]. "Alzheimer's disease. Unravelling the Mystery." National Institute of ageing. National Institutes of Health. 1995.  
<http://www.alzheimers.org/unravel.html> (25 Apr. 2002).
- [5]. "PicksDisease.org." 1999. <http://www.PicksDisease.org> (7 May 2002).
- [6]. "Seeking a Diagnosis – Picks disease."  
<http://www.caringforcarers.net/diagnosis/dic1.html> (7 May 2002).
- [7]. Hietala, Sven-Ola. Nuklearmedicin, Studentlitteratur 1998, Sweden.

- [8]. Imagem SPECT. 1998. <http://dfm.ffclrp.usp.br/fisrad//radio/node65.htm> (6 May 2002).
- [9]. SPECT. 1996. <http://www.bae.ncsu.edu/bae/research/blanchard/www/465/textbook/imaginig/projects/SPECT> (6 May 2002).
- [10]. Koops, W. "A literature study." Philips medical systems. MRI Compendium 1990.
- [11]. Lukban, Andrew. <http://www.bic.mni.mcgill.ca/users/lukban>. (6 May 2002).
- [12]. Newman, Aaron. 1997. <http://www.uoregon.edu/~anewman> (6 May 2002).
- [13]. Huang, Chaorui et. al. "Cingulate cortex hypoperfusion predicts Alzheimer's disease in mild cognitive impairment." Submitted.
- [14]. R. S. J. Frackowiak et. al. "Human Brain Function." San-Diego, CA: Academic Press. 1997.
- [15]. American Psychiatric Association. "Diagnostic and Statistical Manual of Mental Disorders (4<sup>th</sup> ed.)" Washington: American Psychiatric Association. 1994.
- [16]. Radau P.E. et al. "Evaluation of linear registration algorithms for brain SPECT and the errors due to hypoperfusion lesions." Medical Physics 28, p. 1660-1668, Aug 2002.
- [17]. Bevington, Philip R. "Data Reduction and Error Analysis for the Physical Sciences", by McGraw-Hill, Inc. 1969.
- [18]. Press, William H., Teukolsky, Saul A., Vetterling, William T., Flannery, Brian P. "Numerical Recipes in C – The Art of Scientific Computing.", (second edition).
- [19]. Tapiola, Tero. "Biological Markers for Alzheimer's Disease – With Special Emphasis on Cerebrospinal Fluid **b**-Amyloid and Tau." 2001. <http://www.uku.fi/neuro/57the.htm> (27 Apr. 2002).
- [20]. Single object stereology. 2001. <http://www.easymeasure.co.uk/articles/stereology/sos> (7 May 2002).
- [21]. Roberts, N. et al. "The benefit of stereology for quantitative radiology." The British Journal of Radiology, p. 679-695, July 2000.
- [22]. Contextvision – image processing systems. Image Stereology – cvstereo. Software version 1.0. Users guide, revision 1.0. April 1994

[23]. Suckling, J. et al. "A modified fuzzy clustering algorithm for operator independent brain tissue classification of dual echo MR images." *Magnetic Resonance Imaging*, Vol. 17, No. 7, p. 1065-1076, 1999.

[24]. Brandtberg, Tomas. "Introduction to fuzzy sets – with application to image processing and pattern recognition." Centre for Image Analysis, Uppsala University, 1999.

[25]. Brandt, Michael E. et al. "Estimation of CSF, white and grey matter volumes in hydrocephalic children using fuzzy clustering of MR images." *Computerized Medical Imaging and Graphics*, Vol. 18, No. 1, p. 25-34, 1994.

[26]. Lundqvist, M. et al. "Datoriserad bildanalys MN2, Laboration 3." Centrum för bildanalys, Uppsala University. 2001.